

AD-A037 908

RAND CORP SANTA MONICA CALIF

F/G 4/2

A FAST NUMERICAL METHOD FOR EXPLICIT INTEGRATION OF PRIMITIVE E--ETC(U)

JUL 76 M E SCHLESINGER

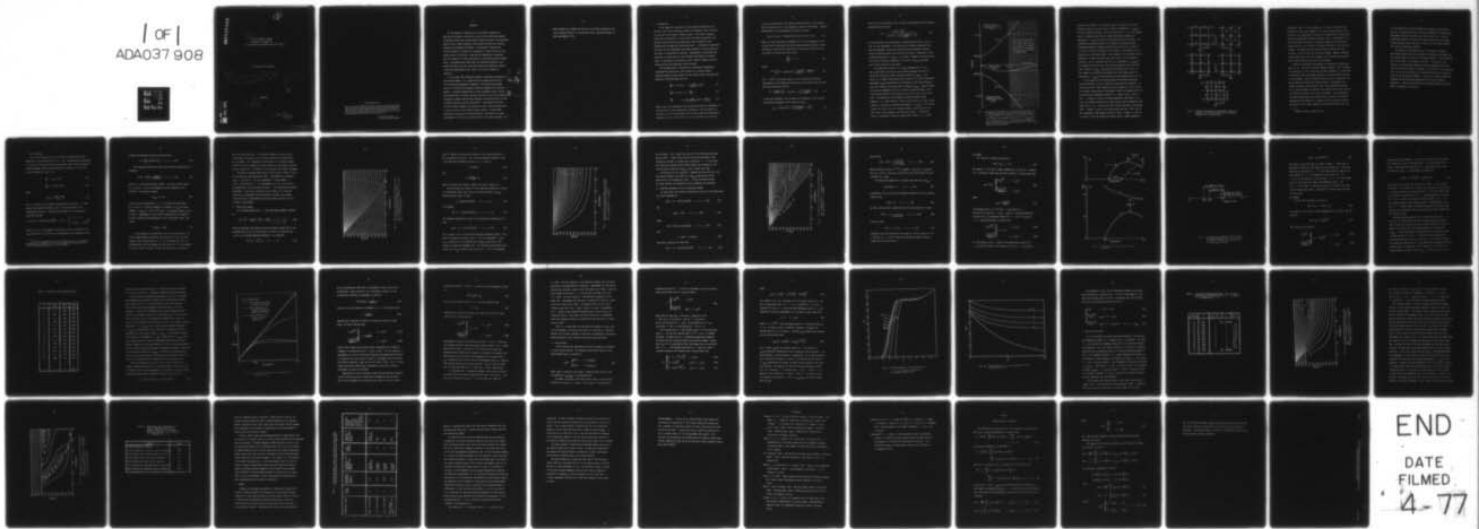
DAHC15-73-C-0181

UNCLASSIFIED

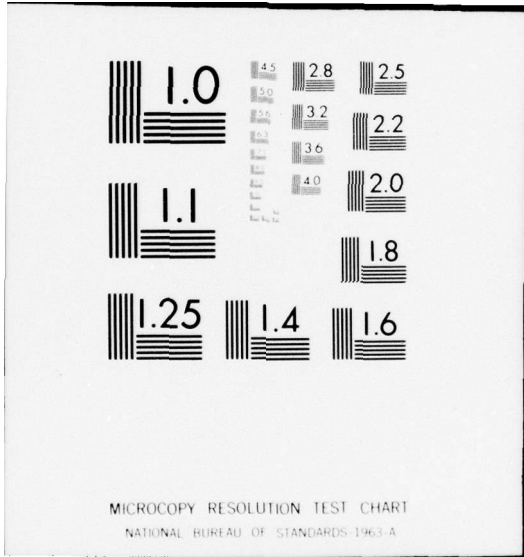
P-5507

NL

1 of 1
ADA037 908



END
DATE
FILMED
4-77



ADA037908

②

⑥

A FAST NUMERICAL METHOD
FOR EXPLICIT INTEGRATION
OF THE PRIMITIVE EQUATIONS NEAR THE POLES,

⑩

Michael E. Schlesinger

⑮

DAHC 15-73-C-4181,
NSF-OCD-75-16923

DDC
APR 8 1976
RECEIVED
C

⑪

July 1976

⑫

52p.

Approved for Release;
Distribution Unlimited

⑭

P-5507

296600

1B

DDC FILE COPY

The Rand Paper Series

Papers are issued by The Rand Corporation as a service to its professional staff. Their purpose is to facilitate the exchange of ideas among those who share the author's research interests; Papers are not reports prepared in fulfillment of Rand's contracts or grants. Views expressed in a Paper are the author's own, and are not necessarily shared by Rand or its research sponsors.

The Rand Corporation
Santa Monica, California 90406

→ hybrid method has allowed the time step of the Rand atmospheric GCM to be increased from six to ten minutes with a resultant decrease in time requirement of 37%.

1. Introduction

In the numerical integration of the primitive equations using explicit time finite difference schemes, the maximum stable time step is governed by the highest frequency waves. The highest frequency waves that are admissible in the primitive system of equations, the external inertia-gravity and Lamb waves, have frequencies that monotonically increase with decreasing scale. In spherical coordinates the scale of any longitudinal wave mode decreases in the direction of the poles as the meridians converge. Consequently, the maximum time step that is stable over the entire sphere (excluding the singular poles) is governed by the smallest scale, highest frequency external inertia-gravity and Lamb waves near the poles.

This problem may be illustrated by considering a homogeneous, incompressible fluid with a free surface on a rotating sphere. Ignoring curvature terms except for the coriolis force, the governing equations linearized about rest are

$$\frac{\partial u}{\partial t} - 2 \Omega \sin \phi v = - \frac{\partial \phi}{a \cos \phi \partial \lambda} S(n), \quad (1)$$

$$\frac{\partial v}{\partial t} + 2 \Omega \sin \phi u = - \frac{\partial \phi}{a \partial \phi}, \quad (2)$$

$$\frac{\partial \phi}{\partial t} = - g H \left[\frac{\partial u}{a \cos \phi \partial \lambda} S(n) + \frac{\partial v}{a \partial \phi} \right], \quad (3)$$

where u and v are respectively the perturbation velocity components in the directions of the longitudinal coordinate λ and latitudinal coordinate ϕ , H and ϕ are respectively the mean height and perturbation geopotential of the free surface, g is the acceleration of gravity,

Ω and a are respectively the rotation speed and radius of the sphere, and the factor $S(n)$ is to be regarded as unity for the moment. Assuming normal modes in the longitudinal direction and time,

$$[u, v, \phi](\lambda, \phi, t) = \text{Re}\{[\hat{u}(\phi), \hat{v}(\phi), \hat{\phi}(\phi)] \exp[i(n\lambda - \omega t)]\}, \quad (4)$$

where n is the longitudinal wavenumber and ω is the frequency, eliminating \hat{u} and $\hat{\phi}$, and making the beta-plane approximation about a fixed latitude ϕ_0 (ignoring the variation of $\sin\phi$ and $\cos\phi$ except for the derivative of the coriolis term) gives

$$\frac{d^2 \hat{v}}{d\phi^2} = -\tau^2 \hat{v}, \quad (5)$$

where

$$\tau^2 = \frac{a^2}{c^2} [\omega^2 - (2\Omega \sin\phi_0)^2] - \left(\frac{n S(n)}{\cos\phi_0}\right)^2 - \frac{2\Omega n S(n)}{\omega}, \quad (6)$$

and $c = (gH)^{1/2}$ is the phase speed of a free surface gravity wave.

Rearranging (6) and dropping the subscript on the beta-plane latitude gives the dispersion relation

$$\omega^2 - \frac{2\Omega n S(n)}{\omega} \left(\frac{c}{a}\right)^2 = (2\Omega \sin\phi)^2 + \left(\frac{c}{a}\right)^2 \left[\left(\frac{n S(n)}{\cos\phi}\right)^2 + \tau^2\right]. \quad (7)$$

In the high frequency limit we obtain the frequency of the eastward and westward propagating inertia-gravity waves,

$$\omega_{IG} = \pm \left\{ (2\Omega \sin\phi)^2 + \left(\frac{c}{a}\right)^2 \left[\left(\frac{n S(n)}{\cos\phi}\right)^2 + \tau^2\right] \right\}^{1/2}, \quad (8)$$

while in the low frequency limit we obtain the frequency of the westward propagating Rossby waves,

$$\omega_R = - \frac{2\Omega n S(n) \left(\frac{c}{a}\right)^2}{(2\Omega \sin\phi)^2 + \left(\frac{c}{a}\right)^2 \left[\left(\frac{nS(n)}{\cos\phi}\right)^2 + l^2 \right]}. \quad (9)$$

As the latitude of the beta-plane is moved toward the poles, $\cos\phi \rightarrow 0$ and, for any wavenumber n , the Rossby wave frequency approaches zero but the frequency of the inertia-gravity waves approaches infinity. Since the maximum stable time step for the explicit integration of the primitive equations is $(\Delta t)_{\max} = \epsilon/\omega$, where ϵ depends on the particular time finite difference scheme but is non-zero, $(\Delta t)_{\max}$ approaches zero in the direction of the poles.

The dispersion relation (7) is shown schematically in Fig. 1. For a prescribed time step Δt , the maximum frequency that will be stable for an explicit time integration scheme is $|\omega|_{\max} = \epsilon/\Delta t$. Unless Δt is chosen sufficiently small, there will be some longitudinal wavenumber $n_{\max}(\phi)$ beyond which the frequency of the inertia-gravity waves will exceed the maximum stable frequency $|\omega|_{\max}$. Several methods are currently employed by various primitive equation general circulation models (GCM's) to overcome the need to use such a small time step. The Geophysical Fluid Dynamics Laboratory (GFDL) model (Manabe *et al.*, 1975) applies a Fourier filter every time step to each prognostic variable to eliminate wavenumbers $n > n_{\max}(\phi)$. This method removes the small scale, low frequency Rossby waves along with the small scale, high frequency inertia-gravity waves. The National Center for Atmospheric Research (NCAR) model (Olinger *et al.*, 1970)

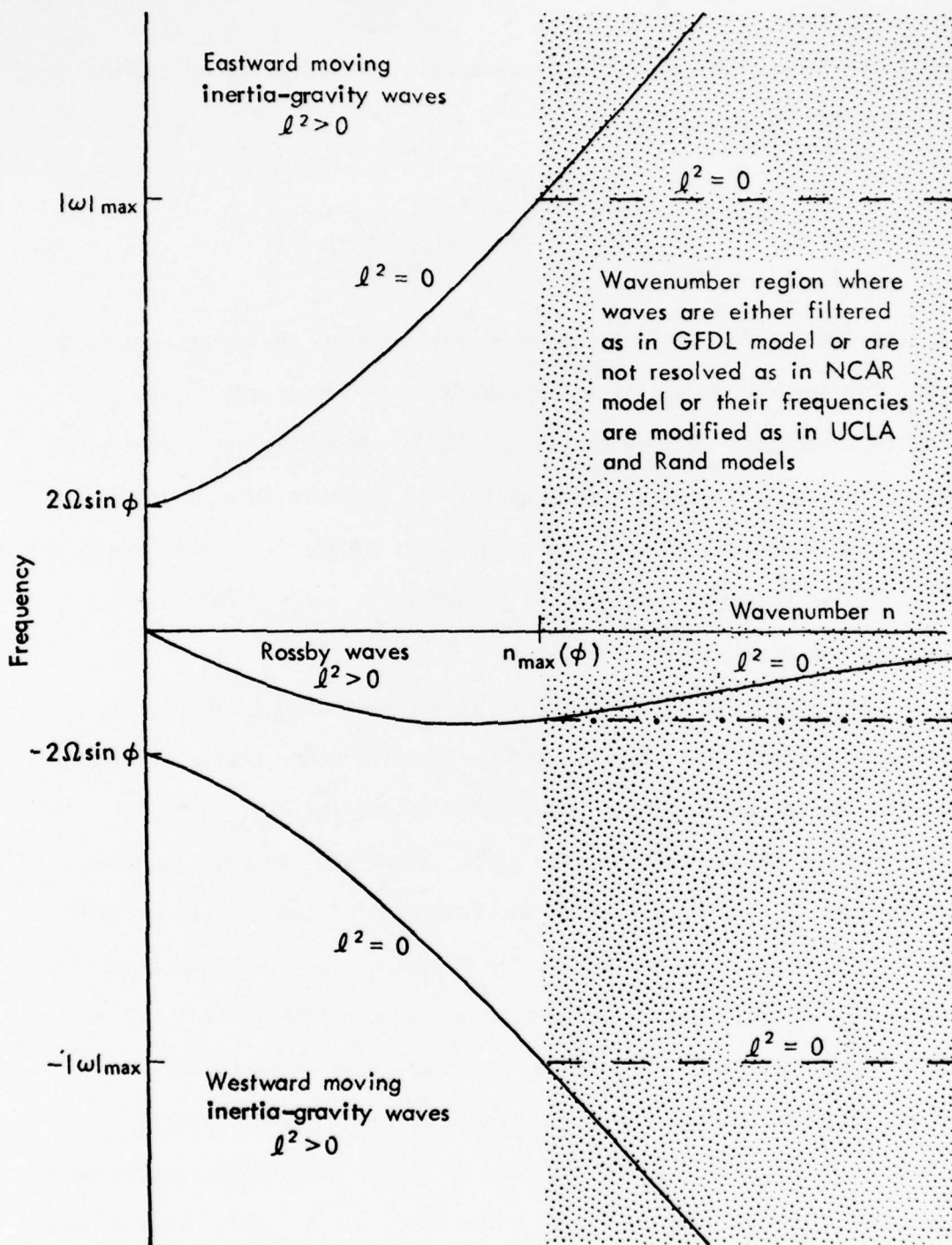


Fig. 1. Schematic representation of the dispersion relation (7). The shading shows the longitudinal wavenumber region $n > n_{\max}(\phi)$ where the frequency of the inertia-gravity waves exceeds the maximum stable frequency $|\omega|_{\max}$ for a prescribed time step Δt . The dashed and dashed-dotted lines illustrate the modified frequencies of the inertia-gravity and Rossby waves.

decreases the number of grid points along a latitude circle in the poleward direction and thus does not resolve wavenumbers $n > n_{\max}(\phi)$. The UCLA (Arakawa and Mintz, 1974) and Rand (Gates *et al.*, 1971) models employ a frequency modification scheme developed by Arakawa for wavenumbers $n > n_{\max}(\phi)$ which are resolved and are not filtered. The longitudinal pressure and mass flux gradients are multiplied by a wavenumber-dependent frequency modification factor $S(n)$ as shown in (1) and (3) for the illustrative fluid system. This modifies, in an energetically consistent manner, the influence of the gradients on the tendencies; it does not modify the actual fields of the prognostic variables. $S(n)$ is defined such that, for wavenumbers $n > n_{\max}(\phi)$, the frequencies given by (8) for the inertia-gravity waves are less than or equal to $|\omega|_{\max}$ (indicated by the dashed lines in Fig. 1); this scheme also modifies the frequencies of the Rossby waves for wavenumbers $n > n_{\max}(\phi)$ (indicated by the dash-dotted line in Fig. 1).

In this paper we only consider models that employ horizontal finite differences in their solution of the primitive equations. In particular we will focus attention on grid schemes B, C and E of the five schemes investigated by Winninghoff (1968) and Arakawa (1972) for distributing the dependent variables on a regular grid as shown in Fig. 2. Scheme B is used in the Rand atmospheric GCM (Gates *et al.*, 1971), the Goddard Institute for Space Studies (GISS) atmospheric GCM (Somerville *et al.*, 1974) and the UCLA oceanic GCM (Mintz and Arakawa, 1974). Scheme C is used in the Rand oceanic GCM (Kim, 1976) and the UCLA atmospheric GCM (Arakawa and Mintz, 1974). Scheme E is used in a version of the Fleet Numerical Weather Central (FNWC) atmospheric

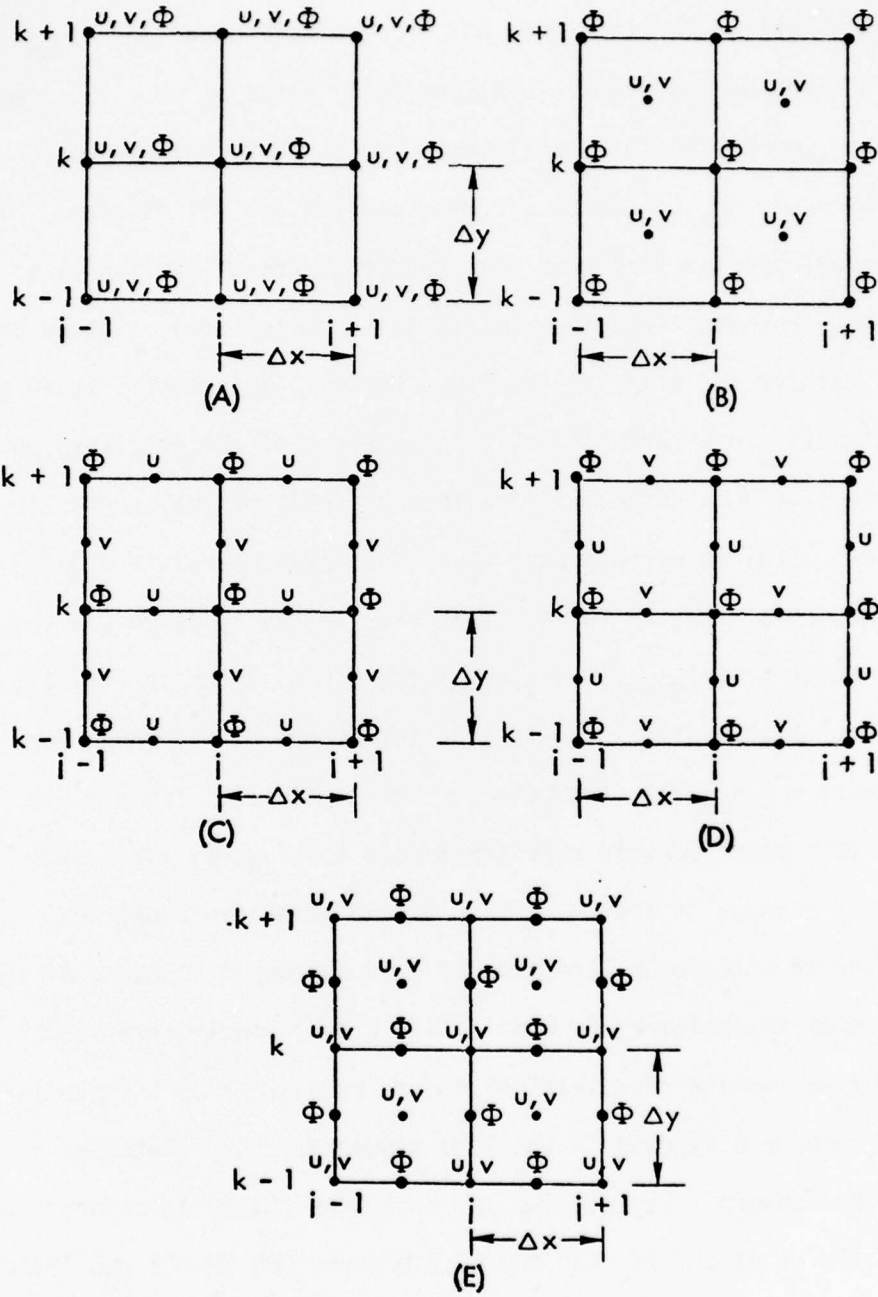


Fig. 2. Schemes investigated by Winninghoff (1968) and Arakawa (1972) for distributing the dependent variables on a regular grid.

GCM (Mihok, 1974). In grid schemes A, B, D and E, contrary to the differential case, the frequency of the inertia-gravity waves at any latitude in two-dimensional flow does not monotonically increase with decreasing wavelength (Arakawa and Mintz, 1974). Furthermore, for a fixed horizontal resolution, the maximum frequency of the inertia-gravity waves at any latitude is different for each of the five grid schemes. This means that the maximum stable time step for each latitude is also different for each grid scheme. However, analogous to the differential case, the frequency of the inertia-gravity waves grows without bound as the poles are approached.

Arakawa has developed two methods, a "three-point" method (see Gates *et al.*, 1971) and a "Fourier" method (Arakawa, 1972), to modify the frequencies of the inertia-gravity waves poleward of a prescribed latitude such that the maximum frequency at the prescribed latitude is not exceeded. Thus the maximum time step that is stable over the entire sphere (excluding the singular poles) is governed by the highest frequency inertia-gravity wave at the prescribed latitude. For a fixed horizontal resolution, this maximum stable time step will be different for each of the five grid schemes. Early experiments by Arakawa showed that the maximum stable time step for the Mintz-Arakawa two-level GCM was six minutes with the three-point method¹. Experiments by the author showed that the maximum stable time step

¹ Arakawa, personal communication.

for this GCM with the Fourier method was increased to ten minutes, but that it required 82% more time than the GCM with the three-point method when both were run with a six minute time step. Thus the three-point method is substantially faster than the Fourier method but the maximum stable time step is larger with the Fourier method than with the three-point method.

The purpose of the present study is to develop a frequency modification method that has the speed of the three-point method and the maximum stable time step of the Fourier method. In the following, the Fourier method is reviewed in section 2. In section 3 the failure of the three-point method to allow the maximum stable time step of the Fourier method is analyzed. In section 4 it is shown that this failure can be overcome by an alternate definition of the parameters of the three-point method. In section 5 a hybrid method that combines the new three-point method with the Fourier method is presented. Finally the application of the hybrid method to several GCM's is presented in section 6.

2. Fourier method

The Fourier method may be illustrated by considering the one-dimensional, non-rotating case of (1) - (3). Introducing the coordinate $x = a\lambda\cos\phi$ and using the simplest second-order space finite difference schemes (Arakawa, 1972), the one-dimensional analogs of (1) and (3) for grid schemes B, C and E² are

$$\frac{\partial u}{\partial t} = - (\delta_x \phi) S(n), \quad (10)$$

$$\frac{\partial \phi}{\partial t} = - c^2 (\delta_x u) S(n), \quad (11)$$

where

$$(\delta_x \alpha)_j = \frac{\alpha_{j+1/2} - \alpha_{j-1/2}}{\Delta x}, \quad (12)$$

and $\Delta x = a\Delta\lambda\cos\phi$ is the variable longitudinal grid length, $\Delta\lambda$ is the angular longitudinal increment, and j is the grid index in the longitudinal direction. Assuming normal modes in the longitudinal direction and time,

$$[u, \phi](j, t) = \text{Re}\{[\hat{u}, \hat{\phi}] \exp[i(\frac{2\pi n}{N} j - \omega t)]\}, \quad \begin{array}{l} j = 1, 2, \dots, N \\ \text{or} \\ j = 1/2, 3/2 \dots, N-1/2 \end{array} \quad (13)$$

where $N = 2\pi/\Delta\lambda$ is the number of grid points along a latitude circle, and eliminating \hat{u} or $\hat{\phi}$ gives for the magnitude of the frequency of the

²
 Δx and N for scheme E must be different from the corresponding quantities for schemes A-D if the total number of grid points in a given two-dimensional domain is to be constant.

eastward and westward propagating gravity waves

$$|\omega| = \frac{2c}{\Delta x} \sin(\pi n/N) S(n), \quad n = 1, \dots, N/2. \quad (14)$$

The frequency modification factor of the Fourier method $S_F(n)$ is defined as

$$S_F(n) = \text{Min} \left[1, \frac{\Delta x/d}{\sin(\pi n/N)} \right], \quad n = 1, \dots, N/2, \quad (15)$$

where d is a prescribed constant length. At (low) latitudes where $\Delta x \geq d$, $S_F(n) = 1$ for all wavenumbers and the frequency is not modified. The maximum frequency

$$|\omega|_{\max} = 2 c/d, \quad (16)$$

occurs at the latitude where $\Delta x = d$. At (high) latitudes where $\Delta x < d$, $S_F(n) \leq 1$ and the frequency is reduced to $|\omega|_{\max}$ for wavenumbers $n > n_{\max}(\phi) = (N/\pi) \sin^{-1}(\Delta x/d)$. The maximum frequency given by (16) is independent of the variable longitudinal grid length Δx . In this illustrative one-dimensional case, the maximum stable time step is

$$(\Delta t)_{\max} = \epsilon \frac{d}{2c}. \quad (17)$$

In the analogous two dimensional case, the maximum stable time step is approximately governed by the analog of (8) for each grid scheme at the latitude where $\Delta x = d$. As illustrated by (17), the maximum stable time step depends on the choice of d . At one extreme, d could be chosen very small so that the frequencies are modified

only very near the poles. At the other extreme, d could be chosen larger than the maximum Δx so that the frequencies are modified at all latitudes. As a compromise, and because it is a natural length scale of the grid, Arakawa has chosen d equal to the constant latitudinal grid length $\Delta y = a \Delta\phi$ where $\Delta\phi$ is the angular latitudinal increment.

The Fourier frequency modification factor $S_F(n)$ is shown in Fig. 3 for the Rand and UCLA atmospheric GCM's. Equatorward of 38 degrees, $\Delta x/\Delta y > 1$ and $S_F(n) = 1$ for all wavenumbers. At 38 degrees, $\Delta x/\Delta y = 0.985$ and $S_F(n) < 1$ for wavenumbers 33 to 36. As the poles are approached, $\Delta x/\Delta y$ decreases and $S_F(n) < 1$ for progressively smaller wavenumbers. $S_F(n)$ has a minimum value of 0.087 (91.3% frequency reduction) at wavenumber 36 and 86 degrees latitude, the maximum latitude where the longitudinal pressure gradient and mass flux are carried in these models.

3. Three-point method

For latitudes where $\Delta x/\Delta y < 1$, the three-point method is defined by

$$f_j^K = f_j^{K-1} + \gamma \left(f_{j-1}^{K-1} - 2f_j^{K-1} + f_{j+1}^{K-1} \right), \quad \begin{array}{l} j = 1, \dots, N; \\ \kappa = 1, \dots, K, \end{array} \quad (18)$$

where f_j^K represents the modified finite difference expression for the gradient $\partial\phi/\partial x$ or $\partial u/\partial x$ at grid point j at the κ -th iteration, and γ and K are latitude dependent parameters. By induction,

$$f_j^K = \left(1 + \gamma\delta^2 \right)^K f_j, \quad j = 1, \dots, N, \quad (19)$$

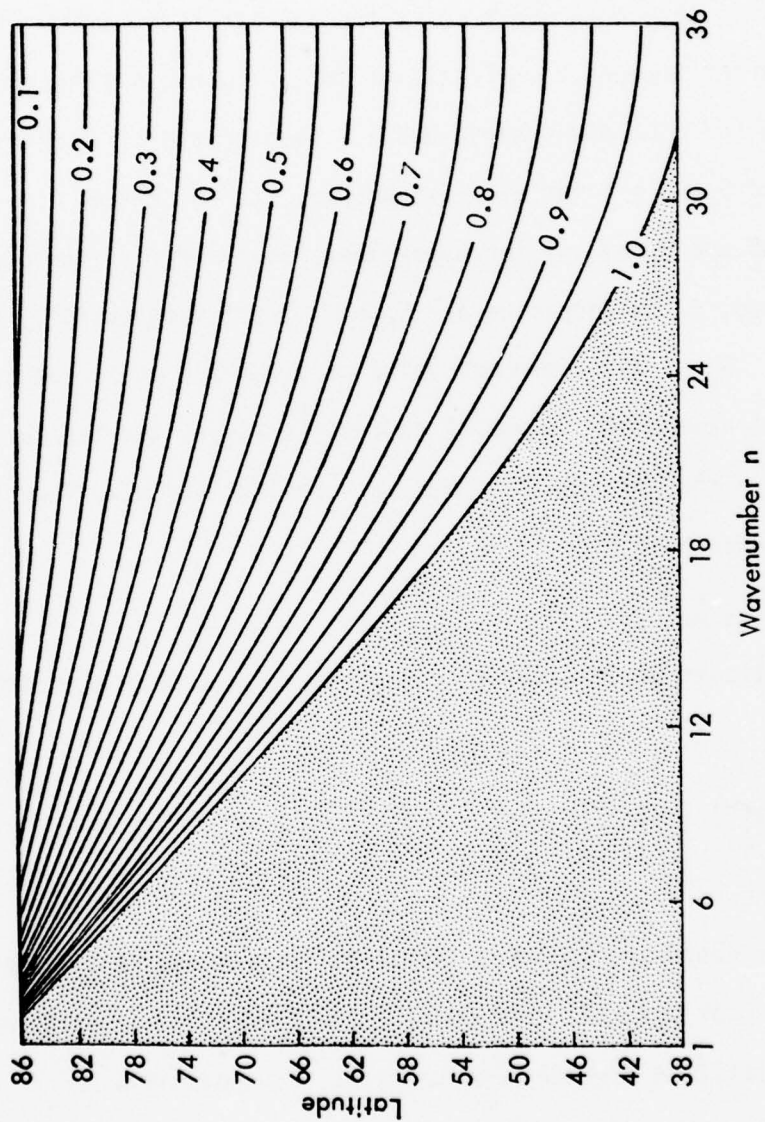


Fig. 3. The Fourier frequency modification factor $S_F(n)$ for the Rand and UCLA atmospheric GCM's ($\Delta\phi = 4$ degrees and $\Delta\lambda = 5$ degrees). The region $S_F(n) \equiv 1$ is shown shaded.

where δ^2 denotes the three-point analog to the second derivative in the longitudinal direction. The latitude dependent parameters K and γ were defined by Arakawa (see Gates *et al.*, 1971) as

$$K = [\Delta y / \Delta x], \quad (20)$$

and

$$\gamma = \frac{(\Delta y / \Delta x) - 1}{8K}, \quad (21)$$

where $[z]$ denotes the largest integer less than or equal to z .

We now analyze the failure of the three-point method to be stable for the maximum stable time step of the Fourier method, $(\Delta t)_{\max}$. Assuming normal modes in space,

$$f_j = \text{Re}\{\exp(i2\pi nj/N)\}, \quad j = 1, \dots, N, \quad (22)$$

(19) becomes

$$f_j^K = [1 - 4\gamma \sin^2(\pi n/N)]^K f_j, \quad j = 1, \dots, N. \quad (23)$$

The frequency modification factor of the three-point method $S_3(n)$ is then

$$S_3(n) = [1 - 4\gamma \sin^2(\pi n/N)]^K, \quad n = 1, \dots, N/2, \quad (24)$$

and is shown in Fig. 4 for the Rand and UCLA atmospheric GCM's. Poleward of 38 degrees latitude, $S_3(n) < 1$ for all wavenumbers. $S_3(n)$ has a minimum value of 0.0008 (99.92% frequency reduction) at 86 degrees latitude and wavenumber 36. For the three-point method to be stable for $(\Delta t)_{\max}$ requires that $S_3(n)/S_F(n) \leq 1$ for all wavenumbers

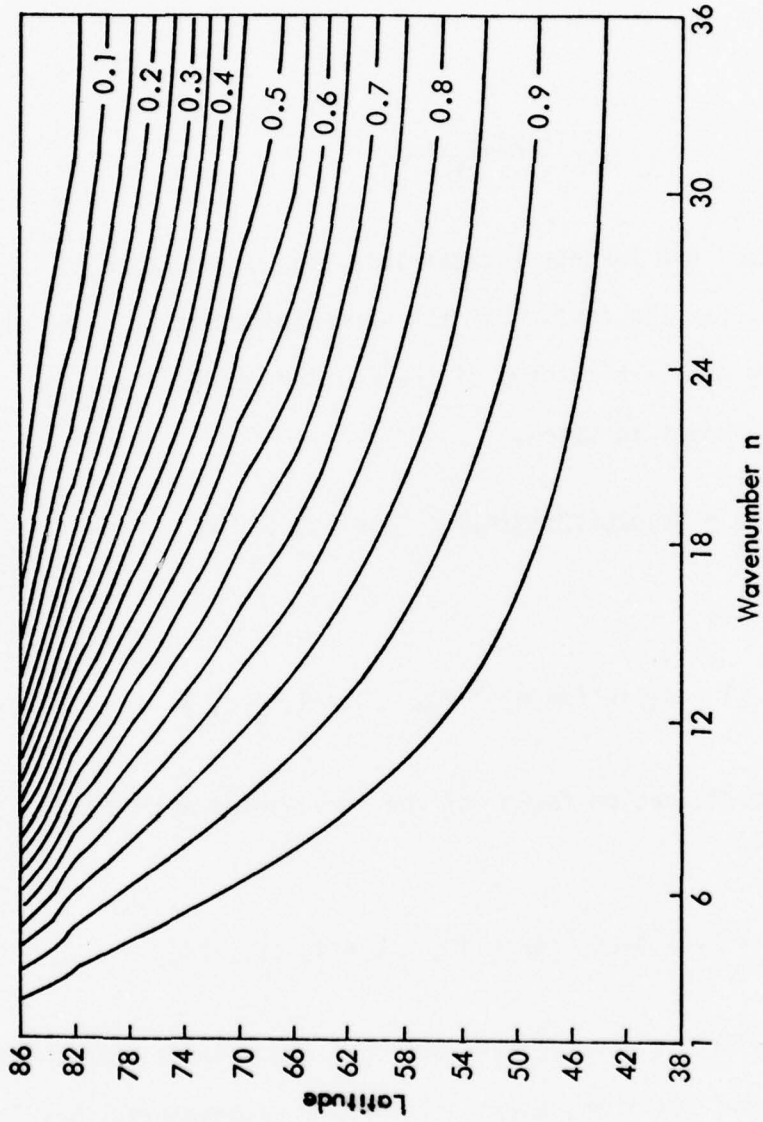


Fig. 4. The three-point frequency modification factor $S_3(n)$ for the Rand and UCLA atmospheric GCM's ($\Delta\phi = 4$ degrees and $\Delta\lambda = 5$ degrees).

and latitudes. Fig. 5 shows $S_3(n)/S_F(n)$ for the Rand and UCLA atmospheric GCM's. A band sloping toward decreasing wavenumbers with increasing latitude is evident where $S_3(n)/S_F(n) > 1$. In this band the three-point method insufficiently reduces the frequency of the inertia-gravity waves for $(\Delta t)_{\max}$ to be a stable time step.

On the basis of this analysis it appears that the failure of the three-point method to be stable for $(\Delta t)_{\max}$ might be due to the definition of the parameters K and γ . In the following section, alternate methods for determining these parameters are presented.

4. Alternate parameters for the three-point method

As shown above the frequency modification factors of the three-point and Fourier methods are

$$S_3(n) = [1 - 4\gamma \sin^2(\pi n/N)]^K, \quad n = 1, \dots, N/2, \quad (25)$$

and

$$S_F(n) = f(n), \quad n = 1, \dots, N/2, \quad (26)$$

where

$$f(n) = \text{Min} [1, r/\sin(\pi n/N)], \quad n = 1, \dots, N/2, \quad (27)$$

and

$$r = \Delta x/\Delta y = \Delta \lambda \cos \phi / \Delta \phi. \quad (28)$$

Defining a function $\Gamma(n)$ such that

$$S_F(n) = [1 - 4\Gamma(n)\sin^2(\pi n/N)]^K, \quad n = 1, \dots, N/2, \quad (29)$$

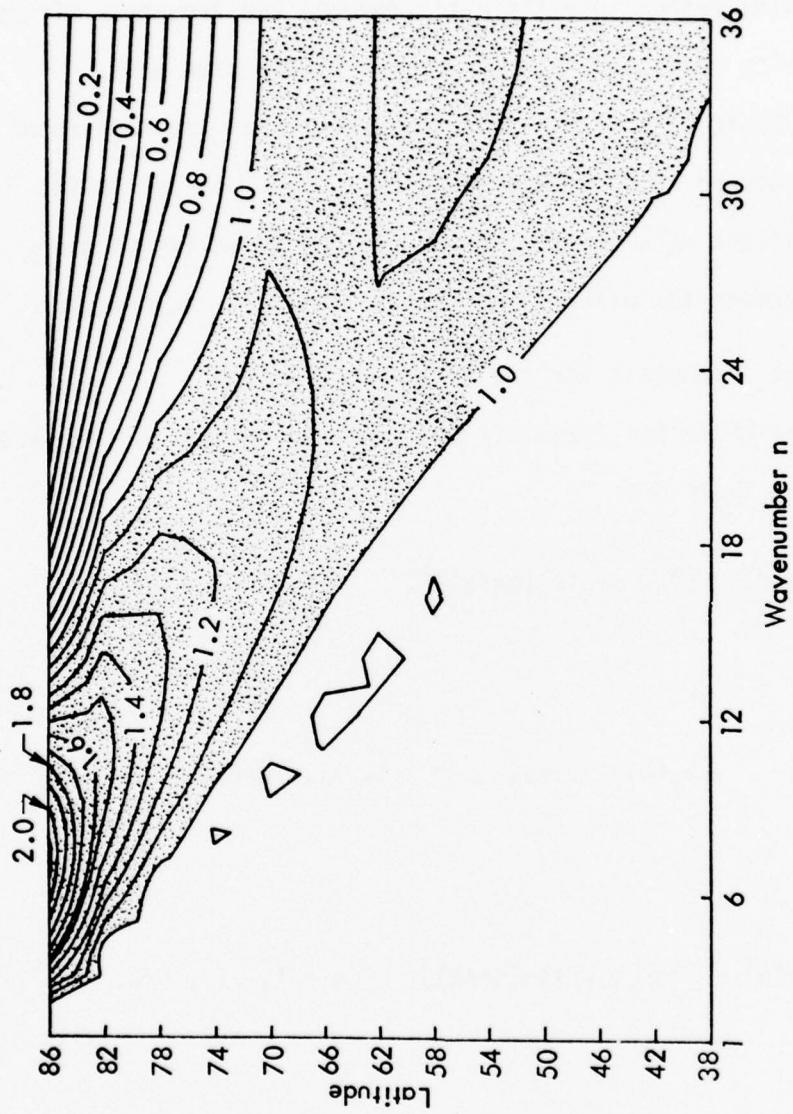


Fig. 5. $S_3(n)/S_F(n)$ for the Rand and UCLA atmospheric GCM's ($\Delta\phi = 4$ degrees and $\Delta\lambda = 5$ degrees). The region where $S_3(n)/S_F(n) \geq 1$ is shaded.

then by (26)

$$\Gamma(n) = \Gamma^{\pm}(n) = \frac{1 \mp f^{1/K}(n)}{4 \sin^2(\pi n/N)}, \quad n = 1, \dots, N/2, \quad (30)$$

where the positive root of $f^{1/K}$ is assumed. Since $S_F(n)$ is positive for all n , $\Gamma^+(n)$ is the only solution for K odd, while both $\Gamma^{\pm}(n)$ are solutions for K even.

The three-point method will be stable with time step $(\Delta t)_{\max}$ if

$$S_3(n)/S_F(n) \leq 1, \quad n = 1, \dots, N/2. \quad (31)$$

Furthermore, for the sign of the modified gradients not to be reversed requires that

$$S_3(n) \geq 0, \quad n = 1, \dots, N/2. \quad (32)$$

By (25), (29) and (30), conditions (31) and (32) require for K odd,

$$\Gamma^+(n) \leq \gamma \leq \frac{1}{4 \sin^2(\pi n/N)}, \quad n = 1, \dots, N/2, \quad (33)$$

and for K even,

$$\Gamma^+(n) \leq \gamma \leq \Gamma^-(n), \quad n = 1, \dots, N/2. \quad (34)$$

Conditions (33) and (34) govern the range of γ and the values of K as a function of r . In the following we investigate these solutions separately for odd and even K .

a. K odd

Eq. (33) for K odd may be written as

$$\text{Max } \Gamma^+(n) \leq \gamma \leq 1/4. \quad (35)$$

The range of γ for K odd is shown schematically in Fig. 6a. Treating n as a continuous rather than discrete variable, it may be shown that

$$\text{Max } \Gamma^+(n) = \begin{cases} \frac{1 - r^{1/K}}{4}, & r \geq r_u(K) \\ \frac{[r_u(K)/r]^2}{4(2K+1)}, & r < r_u(K), \end{cases} \quad (36)$$

where

$$r_u(K) = \left(\frac{2K}{2K+1} \right)^K. \quad (37)$$

The maximum occurs at $n = N/2$ for $r \geq r_u(K)$ and at $n = (N/\pi)\sin^{-1}[r/r_u(K)]$ for $r < r_u(K)$. $r_u(K)$ is a very weak monotonic function for K; it decreases from 2/3 at $K = 1$ to $e^{-1/2} = 0.607$ as $K \rightarrow \infty$. Substituting (36) into (35) gives

$$\left. \begin{array}{l} \frac{1 - r^{1/K}}{4} \\ \frac{[r_u(K)/r]^2}{4(2K+1)} \end{array} \right\} \leq \gamma \leq 1/4 \quad (38a)$$

$$, r < r_u(K). \quad (38b)$$

As illustrated in Fig. 7, (38a) is the appropriate solution for $r \geq r_u(K)$ while (38b) is the solution for $r_m(K) \leq r < r_u(K)$ where

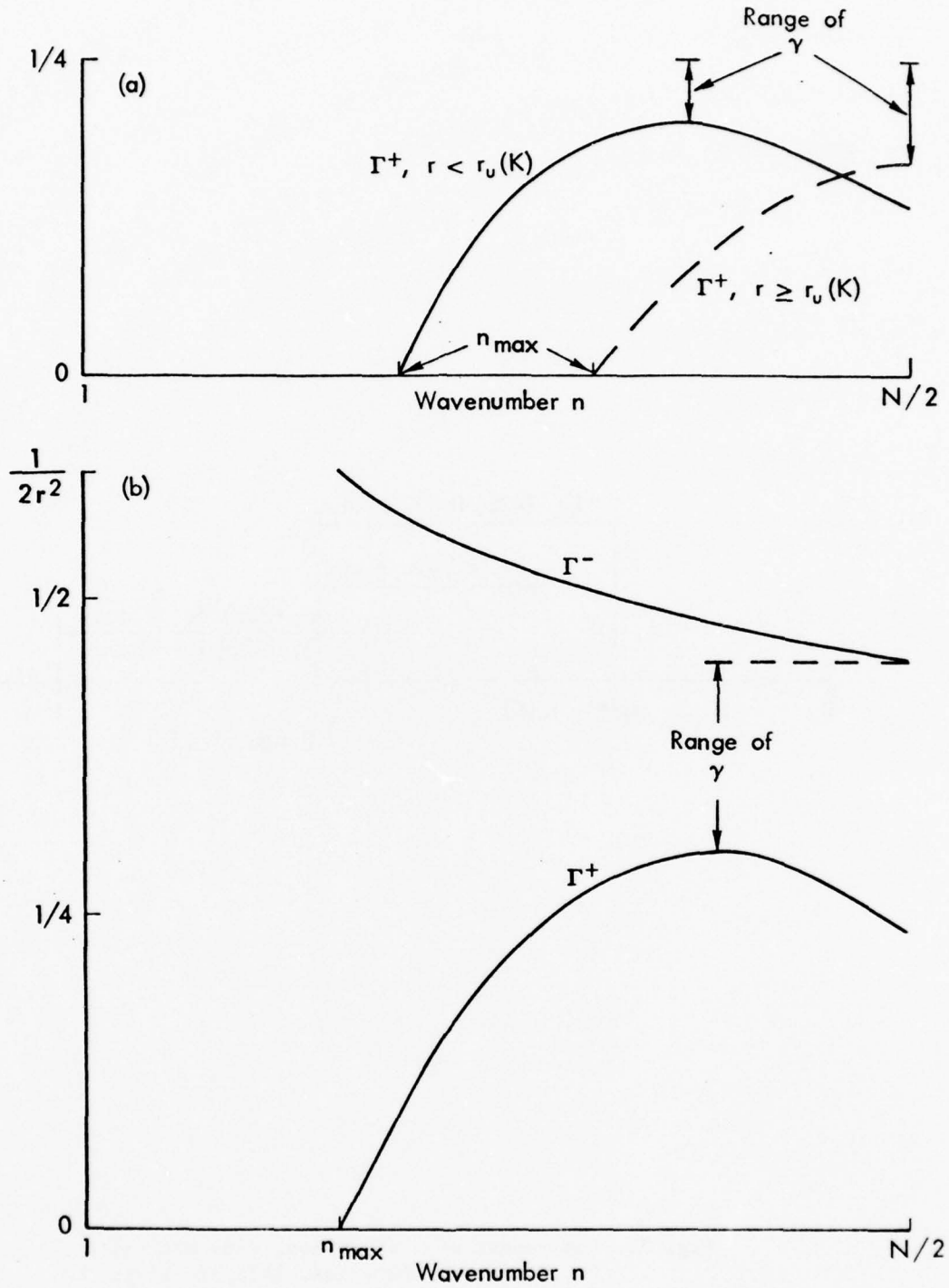


Fig. 6. The range of γ for K odd (a) and for K even (b).

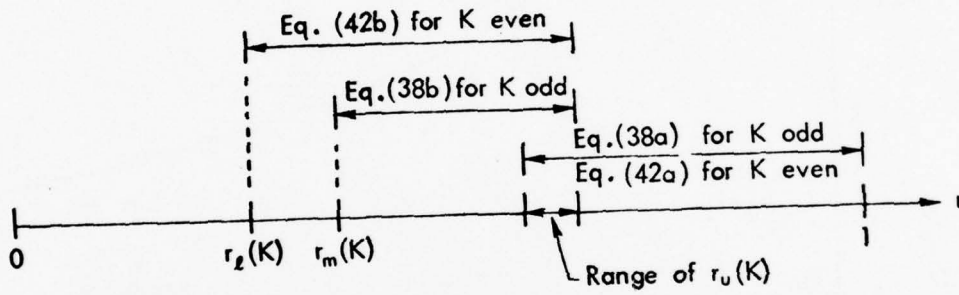


Fig. 7. The ranges of r where Eqs. (38) are valid for K odd and where Eqs. (42) are valid for K even. See text for the definitions of $r_l(K)$, $r_m(K)$ and $r_u(K)$.

$$r_m(K) = r_u(K)/(2K+1)^{1/2}. \quad (39)$$

The values of $r_u(K)$ and $r_m(K)$ are shown in Table 1. Since $r_u(K)$ is bounded by $e^{-1/2}$ and $2/3$, only (38a) can be satisfied for $r > 2/3$, only (38b) can be satisfied for $r < e^{-1/2}$, and either (38a) or (38b) can be satisfied for $e^{-1/2} \leq r \leq 2/3$ depending on the value of K . For $r > 2/3$, all odd values of K satisfy (38a). For $r < e^{-1/2}$, the minimum value of K that satisfies (38b) is determined by $r_m(K)$. For $e^{-1/2} \leq r \leq 2/3$, (38b) is satisfied by values of K smaller than some critical value while (38a) is satisfied by K values larger than this critical value.

b. K even

Eq. (34) for K even may be written as

$$\text{Max } \Gamma^+(n) \leq \gamma \leq \text{Min } \Gamma^-(n). \quad (40)$$

The range of γ for K even is shown schematically in Fig. 6b. By (30) and (27),

$$\text{Min } \Gamma^-(n) = \frac{1 + r^{1/K}}{4}. \quad (41)$$

Thus (40) may be written as

$$\left. \begin{array}{l} \frac{1 - r^{1/K}}{4} \\ [r_u(K)/r]^2 \\ 4(2K+1) \end{array} \right\} \leq \gamma \leq \frac{1 + r^{1/K}}{4} \quad , \quad r \geq r_u(K) \quad (42a)$$

$$, \quad r < r_u(K), \quad (42b)$$

where (36) has been employed. Eqs. (42) for K even differ from (38) for K odd only in their right hand sides. As illustrated in Fig. 7, (42a) is the appropriate solution for $r \geq r_u(K)$ while (42b) is the solution for $r_z(K) \leq r < r_u(K)$ where $r_z(K)$ satisfies

$$r_z(K)[1 + r_z^{1/K}(K)]^{1/2} = r_u(K)/(2K+1)^{1/2}. \quad (43)$$

The values of $r_u(K)$ and $r_z(K)$ are shown in Table 1. Since $r_u(K)$ is bounded by $e^{-1/2}$ and 0.640 (for K even), only (42a) can be satisfied for $r > 0.640$, only (42b) can be satisfied for $r < e^{-1/2}$, and either (42a) or (42b) can be satisfied for $e^{-1/2} \leq r \leq 0.640$ depending on the value of K . For $r > 0.640$, all values of K satisfy (42a). For $r < e^{-1/2}$, the minimum value of K that satisfies (42b) is determined by $r_z(K)$. For $e^{-1/2} \leq r \leq 0.640$, (42b) is satisfied by values of K smaller than some critical value while (42a) is satisfied by K values larger than this critical value.

From the preceding analysis it is evident that for any $r < 1$, there are an infinite number of odd K values that satisfy (38) or even K values that satisfy (42) and, for each value of K , there is a range of γ for which the three-point method will be stable for $(\Delta t)_{\max}$. Clearly additional requirements must be imposed to define a unique solution for γ and K . There are three such additional requirements that we would like to fulfill: (a) similarity between the dispersion characteristics of the modified and unmodified inertia-gravity waves, (b) reduction of the frequency of the waves by the minimum amount required to make $(\Delta t)_{\max}$ a stable time step, and (c)

Table 1. Values of $r_z(k)$, $r_m(k)$ and $r_u(k)$.

k	$r_z(k)$	$r_m(k)$	$r_u(k)$
1	—	.385	.667
2	.235	.286	.640
3	—	.238	.630
4	.163	.208	.624
5	—	.187	.621
6	.131	.172	.619
7	—	.159	.617
8	.113	.149	.616
9	—	.141	.615
10	.100	.134	.614
11	—	.128	.613
12	.091	.123	.613
13	—	.118	.612
14	.084	.114	.612
.	.	.	.
.	.	.	.
.	.	.	.
∞	0	0	.607

selection of the minimum value of K so that the three-point method is as fast as possible in a numerical solution of given resolution.

The difficulty of achieving requirement (a) may be illustrated by considering the dispersion relation for one-dimensional gravity waves shown in Fig. 8. In the differential case, the frequency linearly increases with wavenumber; hence the group velocity is constant. In the finite difference case without frequency modification, the frequency increases with wavenumber more slowly than the linear relation and has an extremum at wavenumber $N/2$; hence the group velocity monotonically decreases to zero at the highest resolved wavenumber. For $(\Delta t)_{\max}$ to be a stable time step when wavenumbers $n > n_{\max}$ are resolved and are not filtered, the frequency must be modified to be less than or equal to $|\omega|_{\max}$. In the Fourier method, the frequency of wavenumbers $n > n_{\max}$ is made equal to $|\omega|_{\max}$; hence their group velocity is zero (in two-dimensional motion the longitudinal component of the group velocity is zero for these wavenumbers). In the original three-point method, the modified frequency is not only too large to be stable with $(\Delta t)_{\max}$, it exhibits an extremum value across which the direction of the group velocity becomes opposite to that of the differential and unmodified finite difference cases.

Since the dispersion relation of the finite difference case without frequency modification is already different from that of the differential case at high wavenumbers, requirement (a) may be defined to mean that the modified frequency given by (14) and (25) as

$$|\omega| = \frac{2c}{\Delta x} \sin(\pi n/N) [1 - 4\gamma \sin^2(\pi n/N)]^K, \quad (44)$$

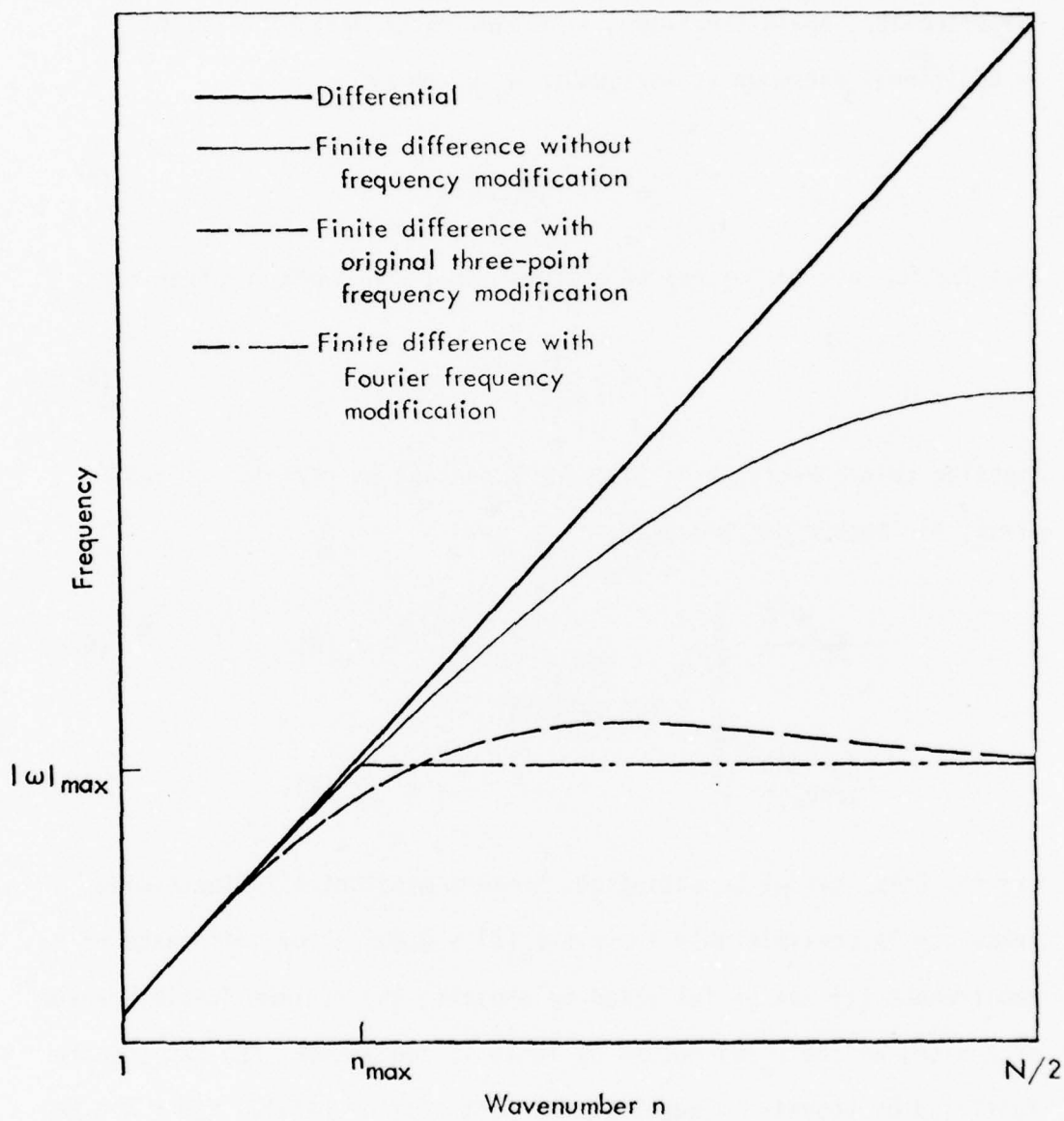


Fig. 8. Dispersion relations for one-dimensional gravity waves.

has no extremum other than that at wavenumber $N/2$ due to the finite differencing. Again treating n as a continuous variable, $|\omega|$ has an additional extremum at wavenumber n_e given by

$$\sin^2(\pi n_e/N) = \frac{1}{4\gamma(2K+1)}. \quad (45)$$

Thus for $|\omega|$ not to possess an extremum in $1 \leq n < N/2$ requires that

$$\gamma \leq \frac{1}{4(2K+1)}. \quad (46)$$

Imposing this constraint on (38) for K odd and on (42) for K even gives, for both K odd and even,

$$\left. \begin{array}{l} \frac{1 - r^{1/K}}{4} \\ [r_u(K)/r]^2 \\ \frac{1}{4(2K+1)} \end{array} \right\} \leq \gamma \leq \frac{1}{4(2K+1)} \quad , r \geq r_u(K) \quad (47a)$$

$$, r < r_u(K). \quad (47b)$$

Clearly (47b) cannot be satisfied, hence a monotonically increasing frequency is possible only for $r \geq r_u(K) \geq 0.607$. For this range of r , requirement (c) can be fulfilled by choosing the minimum possible value of K based on the $r_u(K)$ column of Table 1; requirement (b) can then be fulfilled by choosing γ equal to the left side of (47a). For $r < 0.607$, either the Fourier method must be employed to avoid the extremum or requirement (a) must be redefined.

Requirement (a) may be defined to mean that the modified frequency given by (44) may possess an additional extremum but may not equal zero at any wavenumber (this definition was implicit in the original

three-point method). By (44), $|\omega|$ equals zero at wavenumber n_0 given by

$$\sin^2(\pi n_0/N) = \frac{1}{4\gamma}. \quad (48)$$

For $|\omega|$ not to equal zero in $1 \leq n \leq N/2$ thus requires that

$$\gamma < 1/4. \quad (49)$$

Imposing this constraint on (38) for K odd and on (42) for K even gives for both K odd and even,

$$\left. \begin{array}{l} \frac{1 - r^{1/K}}{4} \\ \\ \frac{[r_u(K)/r]^2}{4(2K+1)} \end{array} \right\} \leq \gamma < 1/4 \quad (50a)$$

$$\left. \begin{array}{l} , r \geq r_u(K) \\ \\ , r < r_u(K). \end{array} \right\} \quad (50b)$$

Requirement (c) may be fulfilled by choosing $K = 1$ for $r \geq 0.667$ and the minimum possible K under the $r_m(K)$ column of Table 1 for $r < 0.667$. Note that for small r , by (39), $K \propto r^{-2}$; hence as the poles are approached many iterations are required to prevent the frequency from equaling zero (for discrete n the frequency will not equal zero if $n_0 \neq$ integer but will be very small for wavenumbers near n_0). Requirement (b) may then be satisfied by choosing γ equal to the left hand side of (50a) and (50b) for $r \geq 0.667$ and $r < 0.667$, respectively.

If requirement (a) is dropped altogether, the fastest version of the three-point method can be obtained from Table 1 as follows. From the $r_u(K)$ column we see that $K = 1$ is sufficient with (38a) for

$r \geq 0.667$. For this range of r , the modified frequency will not equal zero and will be monotonically increasing. Requirement (b) may then be satisfied by choosing γ equal to the left hand side of (38a). From the $r_m(K)$ column we see that $K = 1$ is sufficient with (38b) for $0.385 \leq r < 0.667$. For this range of r , the modified frequency will not equal zero. Requirement (b) may then be satisfied by choosing γ equal to the left hand side of (38b). By comparing the $r_z(K)$ and $r_m(K)$ columns we see that $r_z(K) < r_m(K+1)$ where K is even. Consequently, for $r < 0.385$, we may choose the minimum even K based on the $r_z(K)$ column and select γ from (42b); the precise choice of γ determines where the frequency achieves an extremum (by 45)) and where it equals zero (by (48)).

Since it is undesirable for the modified frequency to equal zero at any wavenumber, and because the number of iterations K required to prevent this rapidly increases as the poles are approached, the hybrid method presented in the following section has been developed.

5. Hybrid method

In this section the three-point and Fourier methods are combined to form a hybrid method. The frequency modification factor of the hybrid method $S_H(n)$ is defined as

$$S_H(n) = \begin{cases} S_3(n), & r \geq r_{\min}(K_{\max}), \\ S_F(n), & r < r_{\min}(K_{\max}), \end{cases} \quad (51)$$

where $S_3(n)$ is given by (25), $S_F(n)$ is given by (26) and (27), and the meaning of $r_{\min}(K_{\max})$ is explained below.

As shown in section 4, the right side of (50) is the necessary condition for $S_3(n) \neq 0$. Since $\gamma < 1/4$, $S_3(n)$ is a monotonically

decreasing function of γ . To fulfill requirement (b) we may therefore choose the minimum value of γ given by (50) as

$$\gamma = \begin{cases} \frac{1 - r^{1/K}}{4}, & r \geq r_u(K) \\ \frac{[r_m(K)/r]^2}{4}, & r_m(K) < r < r_u(K), \end{cases} \quad (52)$$

where (39) has been used. Since (52) is identical to (36),

$\gamma = \text{Max } \Gamma^+(n) = \Gamma^+(m)$ where $m = N/2$ for $r \geq r_u(K)$ and $m = (N/\pi) \sin^{-1}[r/r_u(K)]$ for $r < r_u(K)$. By the definition of $\Gamma^+(n)$, $S_3(n)/S_F(n) = 1$ for $n = m$ and $S_3(n)/S_F(n) < 1$ for $n \neq m$.

For a given value of r , (52) prevents $S_3(n) = 0$ by requiring that $r_m(K) < r$. By (39) this requires that $K \propto r^{-2} \rightarrow \infty$ as $r \rightarrow 0$ towards the poles. At some value of r it therefore becomes more economical to switch from the three-point method to the Fourier method. However, while $S_3(n) = 0$ is prevented by (52), the minimum value of $S_3(n)/S_F(n)$ over $n = 1, \dots, N/2$ becomes quite small as $r \rightarrow r_m(K)$ for fixed K .

Letting M represent this minimum value, it may be shown that

$$M = \begin{cases} \left[1 - (1 - r^{1/K}) r^2 \right]^K, & r \geq r_u(K) \end{cases} \quad (53a)$$

$$\begin{cases} \left[1 - r_m^2(K) \right]^K, & r_p(K) \leq r \leq r_u(K) \end{cases} \quad (53b)$$

$$\begin{cases} \left[1 - (r_m(K)/r)^2 \right]^K \frac{1}{r}, & r_m(K) < r \leq r_p(K), \end{cases} \quad (53c)$$

where

$$r_p(K) = r_m(K) \left\{ 1 - r_p^{1/K}(K) \left[1 - r_m^2(K) \right] \right\}^{-1/2}. \quad (54)$$

M is shown in Fig. 9 as a function of r for several values of K. For any K, M decreases from 1 at r = 1 to $[1 - r_m^2(K)]^K$ at r = r_u(K), is constant for r_p(K) ≤ r ≤ r_u(K), and then approaches zero as r → r_m(K). Therefore, to satisfy requirement (b), we impose a lower bound on M

$$M \geq \delta, \quad r < r_p(K), \quad (55)$$

where $0 \leq \delta < e^{1/2e} = .832$ (the upper bound on δ is given by (53b) as $K \rightarrow \infty$). As shown in Fig. 9, imposing a nonzero δ increases the minimum value of r for a given K. Letting r_min(K) denote this minimum value, (55) and (53c) give

$$r_{\min}(K) = r_m(K) \left[1 - (\delta r_{\min}(K))^{1/K} \right]^{-1/2}. \quad (56)$$

Fig. 10 shows r_min(K) for several values of δ. For nonzero δ, r_min(K) decreases substantially with increasing K only to about K = 10 and thereafter is quasi-constant. Consequently, for a given horizontal grid resolution and nonzero δ, there is an effective maximum value of K, K_max, beyond which no higher latitudes may be treated by the three-point method. For example, for the Rand and UCLA atmospheric GCM's with Δφ = 4 degrees, Δλ = 5 degrees and δ = 0.8, r = .428 at φ = 70 degrees can be treated by K = 5 but r = .345 at φ = 74 degrees cannot be treated by any value of K. For r < r_min(K_max) the Fourier method must be used.

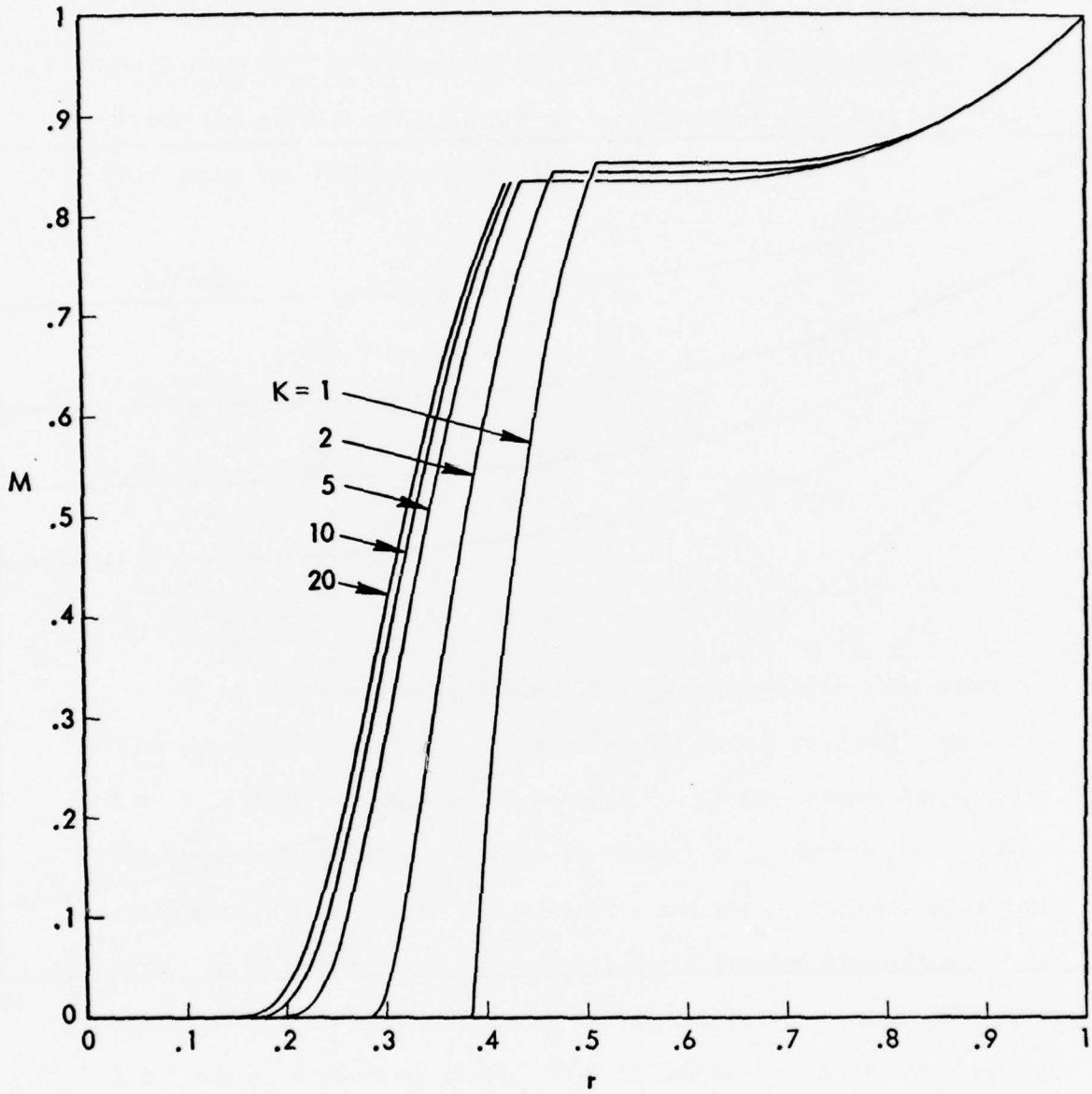


Fig. 9. The minimum value of $S_3(n)/S_F(n)$ over $n = 1, \dots, N/2$ as a function of r for several values of K .

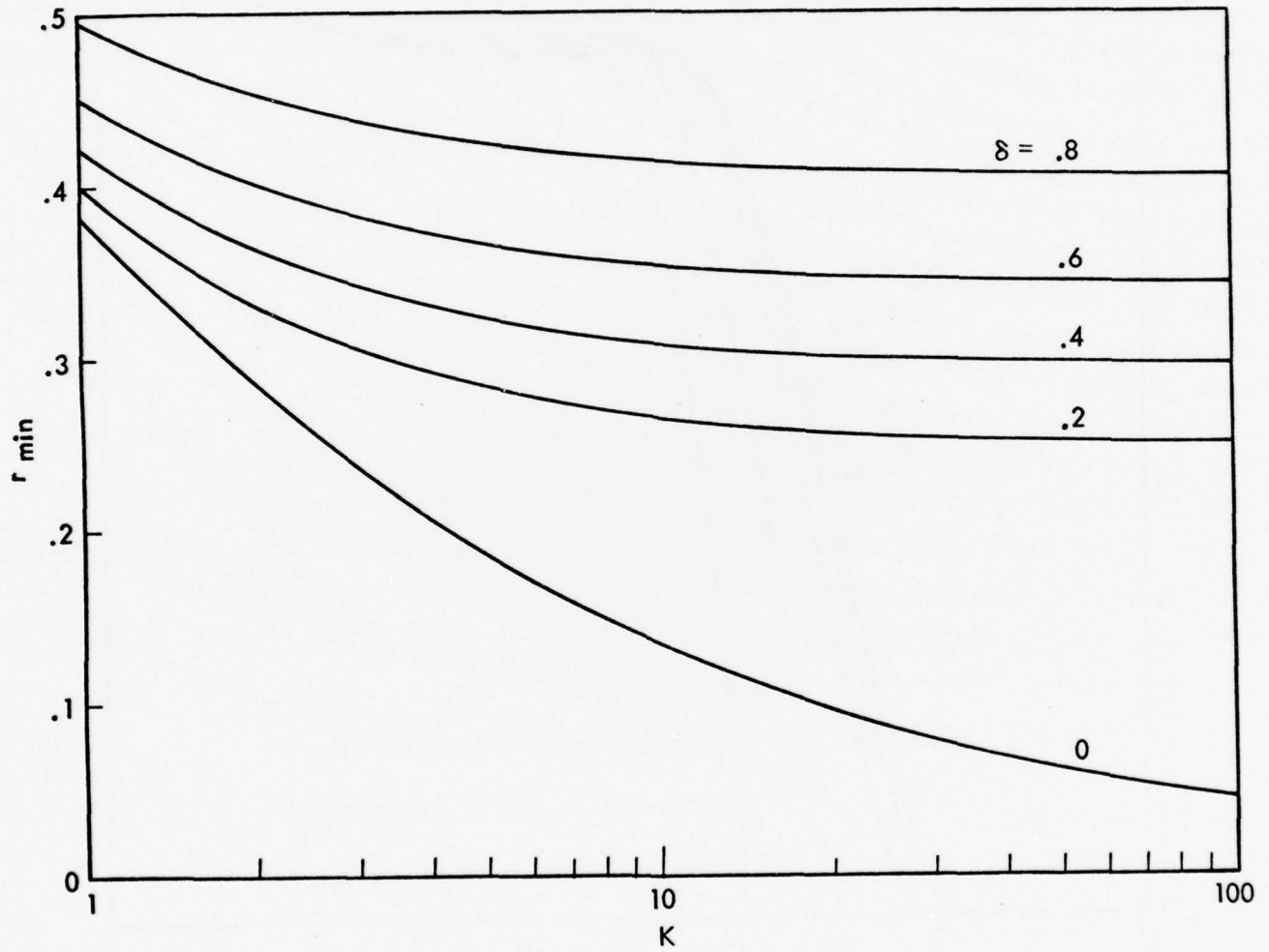


Fig. 10. The minimum value of r as a function of K for several values of δ .

The parameters K and γ for the three-point method can be determined from (52) as a function of r . To fulfill requirement (c), we choose the minimum value of K that is consistent with (52) and (56). This gives the following selection rule for γ :

$$\gamma = \begin{cases} \frac{1-r}{4} & , r \geq r_u(1) = .667 & (57a) \\ \frac{[r_m(1)/r]^2}{4} & , r_{\min}(1) \leq r < r_u(1) & (57b) \\ \frac{[r_m(K)/r]^2}{4} & , r_{\min}(K) \leq r < r_{\min}(K-1), \quad K = 2, \dots, K_{\max} & (57c) \end{cases}$$

6. Application to GCM's

As an illustration we present the hybrid method for the Rand and UCLA atmospheric GCM's ($\Delta\phi = 4$ degrees and $\Delta\lambda = 5$ degrees). We choose $\delta = .8$ to minimize the frequency reduction of the three-point method. The parameters K and γ are shown in Table 2 as a function of latitude along with the corresponding value of r and the appropriate member of (57). At 34 degrees latitude, $r > 1$, hence frequency modification is not required. From 38 degrees to 54 degrees latitude, $r > .667$, hence $K = 1$ and γ is given by (57a). From 58 degrees to 66 degrees latitude, $r > r_{\min}(1) = .495$, hence $K = 1$ and γ is given by (57b). At 70 degrees latitude, $r_{\min}(5) \leq r < r_{\min}(4)$, hence $K = 5$ and γ is given by (57c). At 74 degrees latitude, $r < r_{\min}(\infty)$, hence this and higher latitudes must be treated by the Fourier method.

The frequency modification factor of the hybrid method $S_H(n)$ is shown in Fig. 11 for the Rand and UCLA atmospheric GCM's. Comparison with Fig. 4 for $S_F(n)$ and Fig. 5 for $S_3(n)$ shows that the only

Table 2. Three-point method parameters K and γ for the Rand and UCLA atmospheric GCM's. $\Delta\phi = 4$ degrees, $\Delta\lambda = 5$ degrees and $\delta = .8$.

Latitude	r	Eq. (57)	K	100 γ
34	1.036		NOT	REQUIRED
38	.985	a	1	.375
42	.929	a	1	1.78
46	.868	a	1	3.30
50	.803	a	1	4.92
54	.735	a	1	6.64
58	.662	b	1	8.45
62	.587	b	1	10.8
66	.508	b	1	14.4
70	.428	c	5	4.80
74	.345		NOT	POSSIBLE

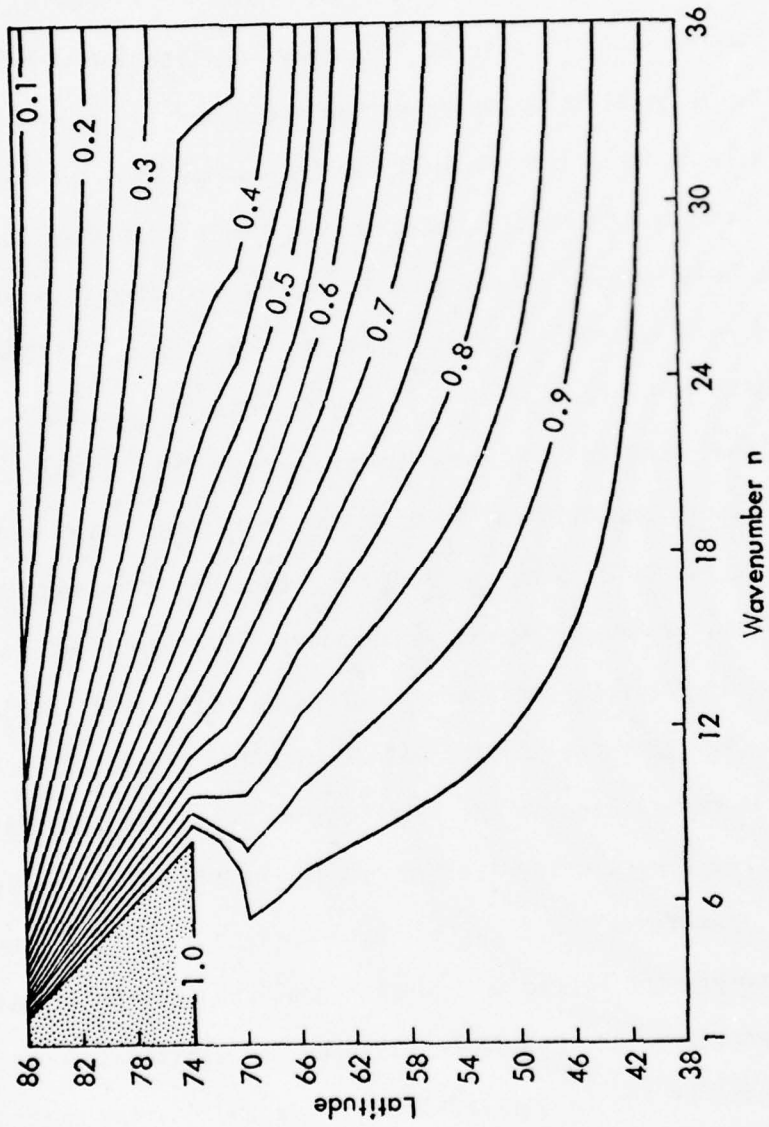


Fig. 11. The hybrid frequency modification factor $S_H(n)$ for the Rand and UCLA atmospheric GCM's ($\Delta\phi = 4$ degrees and $\Delta\lambda = 5$ degrees). The region where $S_H(n) \equiv 1$ is shaded.

qualitative difference is that $S_H(n)$ increases between 70 degrees and 74 degrees latitude for wavenumbers 1 through 9. This occurs because $S_F(n) \equiv 1$ for $n \leq n_{\max}(\phi)$ but $S_3(n) < 1$. Fig. 12 shows that $.8 < S_H(n)/S_F(n) \leq 1$ over the entire latitude-wavenumber domain.

The time requirements of several frequency modification methods relative to the original three-point method are shown in Table 3 for the Rand and UCLA GCM's. The original Fourier method uses a classical Fourier Transform (see Appendix) and is 15.2 times slower than the original three-point method (the Rand atmospheric GCM with this original Fourier method requires 82% more time than the GCM with the original three-point method when both are run with a six minute time step). The hybrid method that combines the three-point method with parameters given in Table 2 and the original Fourier method reduces the time requirement by a factor of two. To further reduce the time requirement, the classical Fourier Transform was replaced by a Fast Fourier Transform. As shown in Table 3, the Fourier method with the Fast Fourier Transform is slower than the Fourier method with the classical Fourier Transform. This occurs because the Fast Fourier Transform transforms all wavenumbers at a particular latitude while the classical Fourier Transform only transforms the required wavenumbers $n > n_{\max}(\phi)$ (see Appendix). However, the hybrid method with the Fast Fourier Transform is slightly faster than the hybrid method with the classical Fourier Transform because, at the (high) latitudes where the Fourier method is used, nearly all wavenumbers must be transformed. As shown in the Appendix, the speed of the classical Fourier Transform can be nearly doubled by a simple improvement. Table 3 shows that the Fourier method

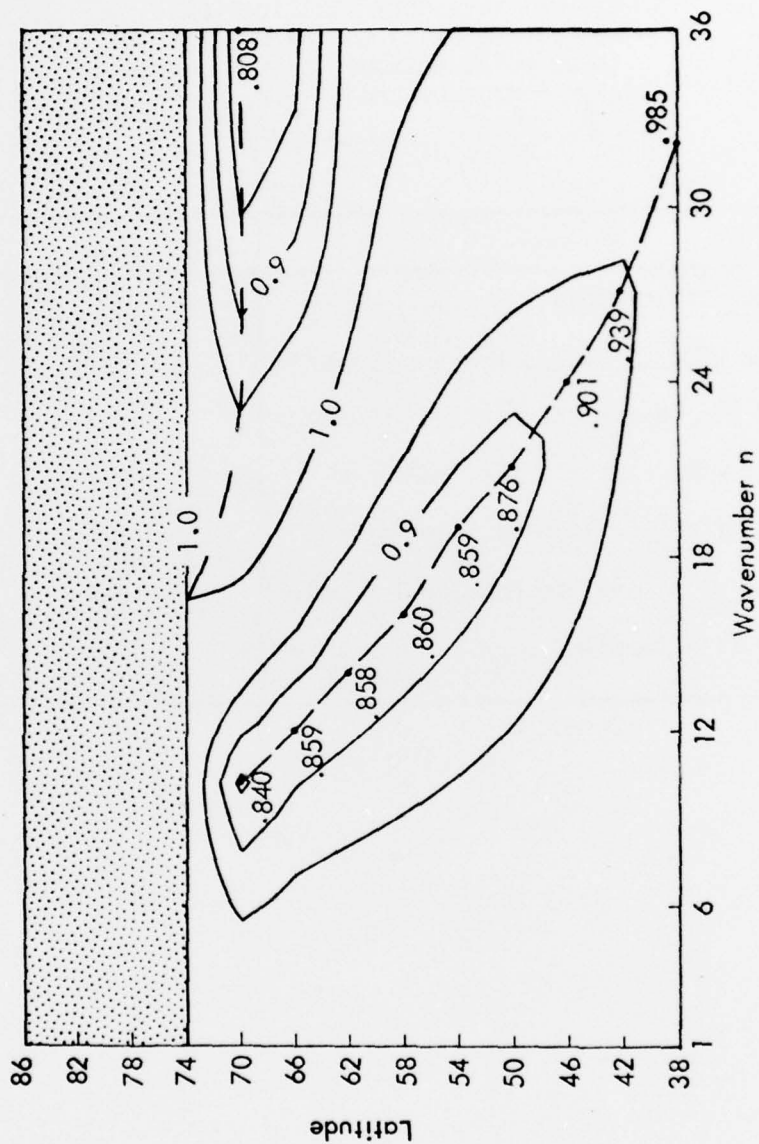


Fig. 12. $S_H(n)/S_F(n)$ for the Rand and UCLA atmospheric GCM's ($\Delta\phi = 4$ degrees and $\Delta\lambda = 5$ degrees). The region where $S_H(n)/S_F(n) \equiv 1$ is shaded and the troughs are dashed.

Table 3. Approximate time requirements of several frequency modification methods relative to the original three-point method. $\Delta\phi = 4$ degrees, $\Delta\lambda = 5$ degrees and $\delta = .8$.

METHOD	TIME
Original Three-Point Method	1
Fourier method with classical Fourier Transform	15.2
Hybrid method with classical Fourier Transform	7.7
Fourier Method with Fast Fourier Transform	19.7
Hybrid Method with Fast Fourier Transform	6.5
Fourier Method with Improved Fourier Transform	8.2
Hybrid Method with Improved Fourier Transform	3.8

with this improved Fourier Transform is almost twice as fast as the original Fourier method and that the hybrid method with the improved Fourier Transform is four times faster than the original Fourier method. Thus, regardless of the Fourier Transform used, the hybrid method is twice as fast as the Fourier method.

Finally, Table 4 shows the percentage decrease in GCM running time for several of the models that are using the hybrid method with the improved Fourier Transform. The Rand atmospheric GCM previously used the original three-point method with its maximum stable time step of six minutes. The hybrid method, while 3.8 times slower than the original three-point method, allows the time step to be increased to the ten minute maximum stable time step of the Fourier method. This results in a 37% decrease in the overall running time. In the other models, the 8.6 - 33% decrease in overall running time results from the fourfold increase in speed of the hybrid method compared to the original Fourier method. (The difference in the percentage decrease in running time for these GCM's is due to differences in their time marching procedures and in their parameterizations of physical processes.)

7. Summary

Arakawa has developed two methods, a "three-point" method and a "Fourier" method to modify the frequencies of inertia-gravity waves poleward of a prescribed latitude such that, without Fourier filtering or reducing the longitudinal resolution, these waves satisfy the linear stability criterion based on the maximum stable time step at the prescribed latitude. Experiments have shown that the three-point

Table 4. Percentage decrease in GCM running time for several models using the hybrid method with improved Fourier Transform.

ATMOSPHERIC MODEL	GRID SCHEME	HORIZONTAL RESOLUTION $\Delta\phi, \Delta\lambda$ (DEGREES)	PREVIOUSLY USED FREQUENCY MODIFICATION METHOD	δ OF HYBRID METHOD	INCREASE IN TIME STEP WITH HYBRID METHOD	PERCENTAGE DECREASE IN GCM RUNNING TIME DUE TO HYBRID METHOD (INCLUDING ANY INCREASE IN TIME STEP)
RAND 2-LEVEL MODEL	B	4,5	ORIGINAL THREE-POINT	.8	FROM 6 TO 10 MINUTES	37
UCLA 12-LEVEL MODEL	C	4,5	ORIGINAL FOURIER	.8	NONE	8.6
FNWC 5-LEVEL MODEL	E	10,10	ORIGINAL FOURIER	.8	NONE	15
MINTZ-ARAKAWA 3-LEVEL MODEL FOR MARS	B	5,6	ORIGINAL FOURIER	.75	NONE	33

method is substantially faster than the Fourier method but that the maximum stable time step is larger with the Fourier method than with the three-point method.

An analysis of the three-point method shows that the modified frequencies of the inertia-gravity waves are too large to be stable with the maximum stable time step of the Fourier method, and suggests that this insufficient frequency reduction is due to the definition of the latitude-dependent parameters K and γ of the three-point method. It is shown that these parameters can be redefined in such a way that the three-point method is stable with the maximum stable time step of the Fourier method; however, this stability requirement alone is not sufficient to determine unique values of K and γ as a function of latitude. These parameters can be uniquely determined by imposing the additional requirements of: (a) similarity between the dispersion characteristics of the modified and unmodified inertia-gravity waves, (b) reduction of the frequency of these waves by the minimum amount required for stability, and (c) selection of the minimum number of iterations K so that the three-point method is as fast as possible. It is shown that the resultant modified frequencies of the inertia-gravity waves do not monotonically increase with wavenumber in high latitudes and that $\gamma < 1/4$ is required to prevent the modified frequencies from becoming zero.

The constraint $\gamma < 1/4$ requires that $K \rightarrow \infty$ as the poles are

approached. At some latitude it therefore becomes more economical to switch from the three-point method with new parameters to the Fourier method. Thus a hybrid method is defined that uses the three-point method at low latitudes and the Fourier method at high latitudes. A selection rule is given for K and γ such that the modified frequency of the three-point method is not less than a prescribed fraction of the modified frequency that would be given by the slower Fourier method.

The hybrid method is stable with the maximum stable time step of the Fourier method and is twice as fast. An additional doubling of the speed of the hybrid method is achieved by a simple improvement of the Fourier Transform used in the Fourier method.

The hybrid method has allowed the time step of the Rand atmospheric GCM to be increased from six to ten minutes with a resultant decrease in time requirement of 37%. The fourfold increase in speed of the hybrid method compared to the original Fourier method has resulted in a decrease in time requirement of 8.6% in the UCLA 12-level atmospheric GCM and 33% in the Mintz-Arakawa 3-level model for Mars.

Acknowledgments. I would like to thank Professor Akio Arakawa for discussing his formulation of the original three-point method and Drs. Jeong-Woo Kim and Mario Juncosa for their discussion during the course of this work. I would also like to express my gratitude to Dr. W. Lawrence Gates for his encouragement and support. This research was sponsored by the Advanced Research Projects Agency under Contract DAHC15-73-C-0181 and by the National Science Foundation under Grant OCD 75-16923.

REFERENCES

- Arakawa, A., 1972: Design of the UCLA general circulation model. Tech. Report No. 7, Numerical Simulation of Weather and Climate, Dept. of Meteorology, University of California, Los Angeles, 116 pp.
- ____ and Y. Mintz, 1974: The UCLA atmospheric general circulation model. Workshop Notes, Dept. of Meteorology, University of California, Los Angeles, 404 pp.
- Gates, W. L., E. S. Batten, A. B. Kahle and A. B. Nelson, 1971: A documentation of the Mintz-Arakawa two-level atmospheric general circulation model. R-877-ARPA, The Rand Corporation, Santa Monica, Calif., 408 pp.
- Kim, Jeong-Woo, 1976: The design of the Rand oceanic general circulation model. P-5511, The Rand Corporation, Santa Monica, Calif. (in preparation).
- Manabe, S., K. Bryan and M. J. Spelman, 1975: A global ocean-atmosphere climate model. Part I. The atmospheric circulation. *J. Phys. Oceanogr.*, 5, 3-29.
- Mihok, W. F., 1974: Global weather prediction model difference schemes, M.S. Thesis, Naval Postgraduate School, Monterey, California, 58 pp.
- Mintz, Y. and A. Arakawa, 1974: The UCLA oceanic general circulation model. Workshop Notes, Dept. of Meteorology, University of California, Los Angeles, 133 pp.
- Olinger, J. E., R. E. Welck, A. Kasahara and W. M. Washington, 1970: Description of NCAR global circulation model. NCAR-TN/STR-56, National Center for Atmospheric Research, Boulder, Colorado, 94 pp.

Somerville, R.C.J., P. H. Stone, M. Halem, J. E. Hansen, J. S. Hogan,
L. M. Druyan, G. Russell, A. A. Lacis, W. J. Quirk and J. Tenenbaum,
1974: The GLISS model of the global atmosphere. *J. Atmos. Sci.*,
31, 84-117.

Winninghoff, F. J., 1968: On the adjustment towards a geostrophic
balance in a simple primitive equation model with application to
the problems of initialization and objective analysis. Ph.D.
Dissertation, Dept. of Meteorology, University of California,
Los Angeles, 161 pp.

APPENDIX

Improved Fourier Transform

The longitudinal pressure and mass flux gradients at longitudinal grid point j may be represented by a Fourier series

$$f_j = \frac{1}{2} A(0) + \sum_{n=1}^{N/2} A(n) \cos\left(\frac{2\pi}{N} nj\right) + \sum_{n=1}^{N/2-1} B(n) \sin\left(\frac{2\pi}{N} nj\right),$$

$$j = 1, \dots, N. \quad (A1)$$

In the Fourier method, f_j is modified to

$$f_j^* = \frac{1}{2} A(0) + \sum_{n=1}^{N/2} S_F(n) A(n) \cos\left(\frac{2\pi}{N} nj\right) + \sum_{n=1}^{N/2-1} S_F(n) B(n) \sin\left(\frac{2\pi}{N} nj\right), \quad j = 1, \dots, N, \quad (A2)$$

where $S_F(n)$ is given by (15). Subtracting (A1) from (A2) gives

$$f_j^* = f_j - \sum_{n=1}^{N/2} [1 - S_F(n)] A(n) \cos\left(\frac{2\pi}{N} nj\right) + \sum_{n=1}^{N/2-1} [1 - S_F(n)] B(n) \sin\left(\frac{2\pi}{N} nj\right), \quad j = 1, \dots, N. \quad (A3)$$

Since $S_F(n) = 1$ for $n \leq n_{\max}(\phi)$, the lower bound of the summations in (A3) should be replaced by $n_{\max}(\phi) + 1$. In the original Fourier method, the coefficients $A(n)$ and $B(n)$ are calculated by the classical Fourier Transform

$$A(n) = \frac{\alpha(n)}{N} \sum_{j=1}^N f_j \cos\left(\frac{2\pi}{N} nj\right), \quad n = n_{\max}(\phi) + 1, \dots, N/2, \quad (A4)$$

$$B(n) = \frac{2}{N} \sum_{j=1}^N f_j \sin\left(\frac{2\pi}{N} nj\right), \quad n = n_{\max}(\phi) + 1, \dots, N/2 - 1 \quad (A5)$$

where

$$\alpha(n) = \begin{cases} 2 & , \quad n \neq N/2 \\ 1 & , \quad n = N/2. \end{cases} \quad (A6)$$

Eqs. (A4) and (A5) together require $2N$ multiplications and $2N-2$ additions for each n .

The speed of this Fourier Transform can be improved as follows.

Writing (A4) and (A5) as

$$A(n) = \frac{\alpha(n)}{N} \sum_{j=1}^{N/2} f_j \cos \left(\frac{2\pi}{N} nj \right) + f_{j+N/2} \cos \left[\frac{2\pi}{N} n(j + N/2) \right],$$

$$B(n) = \frac{2}{N} \sum_{j=1}^{N/2} f_j \sin \left(\frac{2\pi}{N} nj \right) + f_{j+N/2} \sin \left[\frac{2\pi}{N} n(j + N/2) \right],$$

and using the trigonometric relations

$$\cos \left[\frac{2\pi}{N} n(j + N/2) \right] = (-1)^n \cos \left(\frac{2\pi}{N} nj \right),$$

$$\sin \left[\frac{2\pi}{N} n(j + N/2) \right] = (-1)^n \sin \left(\frac{2\pi}{N} nj \right),$$

gives

$$A(n) = \frac{\alpha(n)}{N} \sum_{j=1}^{N/2} g_j(n) \cos \left(\frac{2\pi}{N} nj \right), \quad (A7)$$

$$B(n) = \frac{2}{N} \sum_{j=1}^{N/2} g_j(n) \sin \left(\frac{2\pi}{N} nj \right), \quad (A8)$$

where

$$g_j(n) = \begin{cases} f_j - f_{j+N/2}, & n \text{ odd} \\ f_j + f_{j+N/2}, & n \text{ even.} \end{cases} \quad j = 1, \dots, N/2 \quad (A9)$$

Eqs. (A7) and (A8) together require N multiplications and $N-2$ additions for each n , and the calculation of the N different $g_j(n)$ requires N additions. The improved Fourier Transform is thus almost twice as fast as the classical Fourier Transform.

P-5507

A FAST NUMERICAL METHOD FOR EXPLICIT INTEGRATION OF THE
PRIMITIVE EQUATIONS NEAR THE POLES

Schlesinger